Estudo numérico e experimental do impacto lateral em componentes feitos de material composto

Numerical and experimental study of the lateral impact on composite components

Abstract

The main part of the present project plan (2023-2024) is related to the 'part d: Dynamic friction coefficient' mentioned in the project plan for 2022-2023. The friction between two surfaces affects structural deformation mode and kinetic energy absorption capacity during accidents and collisions. Dynamic friction has not received sufficient attention in the area of automotive crashworthiness. The lack of knowledge on contact friction data of different materials, like metallic parts of automobiles, airbags, seat belts, dummy skin, and so on has affected the reliability and predictability of vehicle crash simulations. Thus this project aims to conduct a comprehensive study to expand our knowledge of friction coefficient factors between a large variety of materials in the automotive industry. The specimens, dummy skins, seat covers, seat belts, metallic parts, and honeycomb components are provided by BMW company.

Besides the main part of this project plan, there are several minor projects including material characterization tests and high-energy impact tests that should be conducted for companies and institutes during this year (2023).

Keywords: Crashworthiness; impact simulation; sliding friction.

1. Introduction

In a vehicle crash surfaces of the interior and exterior parts of the vehicle and occupant undergo unique and complex dry sliding friction. Contact friction plays a crucial role in vehicle crash-worthy performance. Although dissipated kinetic energy by friction is of a small amount, the friction can indirectly affect the vehicle's crashworthiness by affecting the deformation modes [1]. In vehicle crash simulation (FE models), the contact friction shall be simulated with adequate accuracy to ensure the reliability of FE models. However, friction coefficients in numerical models are commonly assumed based on experience, and sometimes even served as a tuning parameter for improving the correlation between simulation and test results [2]. The sliding friction in vehicle crashes has received less attention and it seems there is a lack of knowledge and data on the friction behavior of different materials of exterior and interior parts of a vehicle.

During a vehicle crash, the contact condition between different surfaces is different. It is important to note that both pressure and velocity between two contact surfaces are not constant during crash development [3]. Tables 1 and 2 listed the slip rate and pressure between different parts (interior and exterior parts) during a crash FE simulation [3].

Pressure (MPa)	Aluminium bumper	Dummy head	Dummy chest
Max	405.09	3.48	15.31
Mean	106.64	0.34	6.76
Std	68.09	0.80	4.88
Min	0.02	0.00	0.00

Table 1. Pressure levels during a crash test for different parts.

Slip rate (m/s)	Dummy head–airbag	Seatbelt–dummy shirt	Airbag–seatbelt	Airbag–dummy shirt
Max	40.87	5.12	0.55	5.55
Mean	18.98	0.92	0.19	2.52
Std	10.05	1.61	0.14	1.21
Min	4.35	0.00	0.04	0.26

Table 2. Slip rate levels during a crash test for different parts.

There are a variety of tribometers (instruments for measuring friction in sliding) that are being widely used for measuring dynamic friction under relatively high contact pressure (1-35 MPa) and sliding velocity (1-10m/s) [4], [5].

This study aims to experimentally characterize the friction properties in dry sliding between a large variety of materials, metallic sheets, rubber of dummy skin, seatbelt, and seat cover under different sliding rates (quasi-static to higher velocities up to 3 m/s) and contact pressures close to those in vehicle crashes.

2. Experimental procedure and specimens

2.1 Experimental procedure

The friction test rig (as shown in Fig. 1) was developed by [3] in the GMSIE laboratory to investigate the sliding friction of hard and soft materials under different normal forces (pressures) and static to high relative velocities.

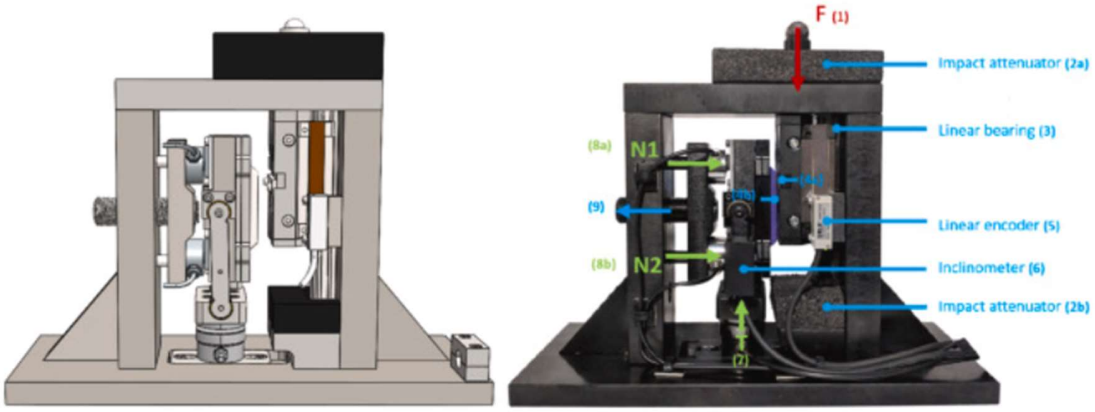

(a)

(b)

(c)

Fig. 1. Sliding friction test rig; (a) Description of the rig, (b) friction rig on the quas-static machine, and (c) Friction rig on the drop hammer facility.

2.2 Required equipment

Seral pieces of equipment available in the GMISE laboratory will be used to conduct the tests. Some pieces of equipment are listed as follows

- High-speed camera
- Fyldes strain gauge bridges, for load cells o the friction rig
- Ni DAq boards and applications like LabView and Matlab
- Instron quasi-static universal testing machine
- Low-energy drop hammer test facility

2.3 Specimens

A large variety of specimens from different materials, like metals, rubbers, and textiles, are provided by BMW to be tested. Figure 2 illustrates the materials for the present study.

Fig. 2. Materials for the friction study.

The friction behavior between pairs of similar and nonsimilar surfaces will be investigated under high contact pressures and velocities. Applying high pressure on softer materials like rubbers (dummy skin) is a big challenge in the present study similar to many other studies that the misalignment problem between the interacting flat surfaces is frequently observed [6].

The performance and validity of friction rig are investigated Ref [3] for several soft materials. This reference will be the guideline for performing the experimental friction tests in the present study.

3. Minor projects for the 2023-2024 academic year

The post-doc student is responsible for all experimental tests that should be conducted during the period of the project. A few projects are already assigned to the Pos-doc student as follows

- PA: Material characterization of TRIP and DP steels for Senai-Fiat
  - Tehsile high-strain rate (using Split Hopkinson's tension bar)
  - Quas-static tensile test
  - Finding Johnson-Cook plasticity parameters, A, B, n, and C.

- PB: Material characterization and impact test on the energy absorber
  - High-strain rate compression and tension tests (using SHTB and SHPB)
  - Impact on the energy absorbers using high-energy drop hammer at GMSIE laboratory.

4. Activities and timetable

The research duration is divided into four periods (four three), P1, P2, P3, and P4 as listed in the following timetable.

- Activities related to the sliding friction investigation (main project):

A1. Planning and making designs for cutting required samples from raw materials,

A2. Finding more desired methods for attaching the specimens to the friction rig, preventing misalignment,

A3. Conducting preliminary tests for checking the rig, equipment, and instruments,

A4. Performing the quasi-static friction tests,

A5. Performing the high-velocity friction tests, and

A6. Data reduction and preparing the final report.

- Activities related to the PA project (additional project):

PA1. Designing tensile specimens for QS and high-strain tensile tests,

PA2. Conducting quasi-static tensile test,

PA3. Conducting high-strain rate tensile tests using SHTB,

PA4. Obtaining the JC plasticity model parameters,

PA5. Preparing final report.

- Activities related to the PB project (additional project):

PB1. Preparing the specimens, after receiving the raw materials and components,

PB2. Material characterization at high-strain rates using SHTB and SHPB.

PB3. Preparing and conducting axial impact tests on the energy absorbers using the high-energy drop hammer rig.

Table 3. Timetable.

Activity	P1	P2	P3	P4
PA3, PA4, PA5,A1, A2				
PB1,PB2,PB3				
Publishing paper from Embraer tests		*		
A3, A4				
A5, A6				
Publications				

* The draft of the manuscript for a journal paper is ready, however, since the test results are applied for European safety certification (under analysis); waiting for Embraer's permission to be able to submit the paper.

5. Project progress and accomplishments

	Academic year			
	2020	2021	2022	2023
Progress				

	Description	Achievement
	Strat the lateral ballistic impact test on composite and aluminum plates Deu to the pandemic access to the lab was partially or restricted, thus working on developing an FE model of impact on composite and aluminum plates and designing a new gas gun at the GMSIE lab	New light gas gun+ measurement equipment and transparent bulletproof safety box Two papers on FE modeling CFRP materials using user-material subroutine
	Conducting experimental tests including high-strain rate material characterization and lateral impact on the polymeric sleeper (full scale) at room and (– 30 °C) temperature	Finalizing project for Braskem petro-mechanical company Presenting 2 conference papers (2022) Preparing a journal paper (submitted 2023)
	Conducting ballistic impact tests for Embraer (for obtaining Europan safety certifications) Conducting an additional study with Prof. Tita (Structural health monitoring)	Finalizing the ballistic tests Presenting a conference paper on SHM (2022)
	Performing extra ballistic impact tests on aluminum plates to write a paper manuscript Validating and improving the numerical model of impact on the sandwich composite panel and aluminum plate using experimental results Writing a draft of the paper Preparation for sliding friction tests	The draft of the manuscript is ready, waiting for Embraer permission to be submitted

References

[1] A. Alavi Nia and J. Haddad Hamedani, “Comparative analysis of energy absorption and deformations of thin walled tubes with various section geometries,” *Thin-Walled Struct.*, vol. 48, no. 12, pp. 946–954, Dec. 2010.

[2] X. Lai, Y. Xia, X. Wu, and Q. Zhou, “An experimental method for characterizing friction properties of sheet metal under high contact pressure,” *Wear*, vol. 289, pp. 82–94, Jun. 2012.

[3] B. Mussulini, L. Driemeier, R. T. Moura, R. T. Vargas, H. Ramos, and M. Alves, “Slip rate and pressure sensitive friction measurement for crash simulation,” *Int. J. Impact Eng.*, vol. 176, p. 104573, Apr. 2023.

[4] W.-R. Chang *et al.*, “The role of friction in the measurement of slipperiness, Part 2: Survey of friction measurement devices,” *Ergonomics*, vol. 44, no. 13, pp. 1233–1261, Oct. 2001.

[5] G. Pürçek, T. Savaşkan, T. Küçükömeroğlu, and S. Murphy, “Dry sliding friction and wear properties of zinc-based alloys,” *Wear*, vol. 252, no. 11–12, pp. 894–901, Jul. 2002.

[6] J. E. Dunkin and D. E. Kim, “Measurement of static friction coefficient between flat surfaces,” *Wear*, vol. 193, no. 2, pp. 186–192, May 1996.

Appendix I: Submitted paper to International Journal of Rail Transportation

Title: Dynamic Response of Polymeric Railway Sleepers under Harsh Loading and Environmental Conditions

Status:

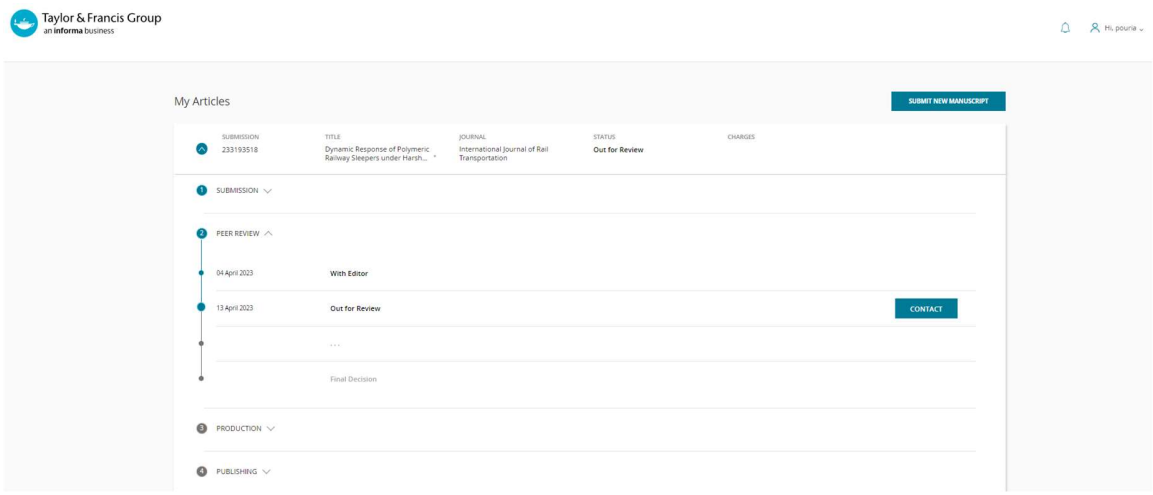

Conference papers

- Polymeric sleepers a new development methodology, 6th BccM
- Impact response of polymeric train sleepers, Mecsol 2022, Campinas.
- Structural Health Monitoring of Thermoplastic Composite Beams via Vibration-based Method, Mecsol 2022, Campinas.

Journal paper based on Embraer test results + simulation

The draft of the manuscript is ready, however, since the test results are applied for European safety certification (under analysis); I have to wait for Embraer's permission to be able to submit the paper.

The draft version of the manuscript

Dynamic Response of Polymeric Railway Sleepers under Harsh Loading and Environmental Conditions

P.B. Ataabadi[1], Renato Vargas[2], and M. Alves[1]

[1] University of Sao Paulo, Group of Solid Mechanics and Structural Impact, Department of Mechatronics and Mechanical Systems Engineering, Sao Paulo 05508900, Brazil

[2] University of Sao Paulo, Sao Paulo 05508900, Brazil

Abstract

High-magnitude impact loads can occur on the railway track and sleepers due to wheel/rail abnormalities or train derailment. Several polymeric composite sleeper technologies have been developed and the railway sector is replacing old fashion sleepers with composite ones; however, the behavior of composite sleepers under impact loading has not been comprehended yet. In the present paper, a high-energy drop hammer test facility was utilized to investigate the impact behavior of a polymeric composite railway sleeper. Due to the temperature and strain rate dependency of the thermoplastic materials of the sleepers, besides the impact test at room temperature (~ 23°C) impact tests at extremely low temperatures (~ minus 30°C) were performed on the sleepers. Quasi-static and high strain rate tests on the materials at room temperature and low/elevated temperatures were conducted to reach more insight into the temperature and strain rate effects on the mechanical properties of materials. The results can be used for finite element analysis purposes so the design of polymeric sleepers can be performed and improved as an alternative for traditional materials like timber and concrete.

Appendix II: Embraer final report (Only experimental tests, results are removed here)

Final report
Fuel Tank Small Debris Impact Test

Experimental tests were conducted by

Pouria Bahrami Ataabadi

Matheus Ferreira

Supervised by

Prof. Dr. Marcilio Alves and Embraer team

GMSIE LABORATORY

OCTOBER 2022

Contents

Abstract

The present study aimed to investigate the strength of metallic fuel tank stub panels when submitted to small cubic debris impact as required by European Aviation Safety

Agency, EASA. Several impact tests with two different configurations; (I) First configuration: a projectile first impacts a composite sandwich panel then impacts an aluminum plate, (II) Second configuration: The projectile directly impacts the aluminum plate. Different thicknesses of aluminum plates were tested to find the minimum thickness that can meet leakage test criteria. The effect of different impact orientations of cubic projectiles was investigated.

Keywords: Cubic projectile; leakage test; gas gun; impact orientation.

Specimens and projectile for the impact test

Here in this section specimens, projectiles, and general conditions of impact tests are explained briefly.

Specimens and impact configurations

There are two types of specimens (targets) in this study; (I) honeycomb sandwich square panel and (II) Aluminum Al 7475-T7351 plates with different thicknesses. The sandwich panel is made of four layers of Carbon M92S fabric with 0.239 mm each (skins) and one Honeycomb Nomex core with 12.604 mm [1].

Two impact configurations were considered in this study; (I) First impact configuration: in the first configuration the projectile first impacts the sandwich panel then the projectile hit the aluminum plate that was fixed 200 (mm) away from the sandwich panel, (II) Second impact configuration: in the second configuration the sandwich panel was removed and the projectile directly hit the aluminum plate. All measurements such as velocity measurement and impact angles verification were done before the first impact. Figure 1 illustrates these two configurations schematically. The first configuration was the main part of the study, thus this configuration had been investigated more extensively rather than the second impact configuration.

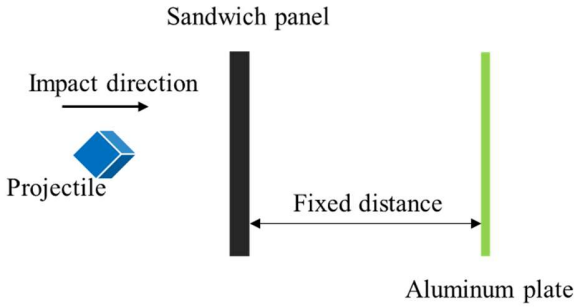

(a): First configuration

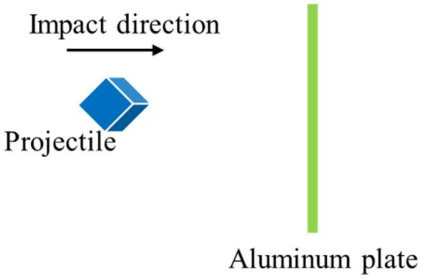

(b): Second configuration

Fig.1 – Two different impact configurations.

Figure 2 shows the photographs of the sandwich composite panel and an aluminum plate, for more details see Ref. [1].

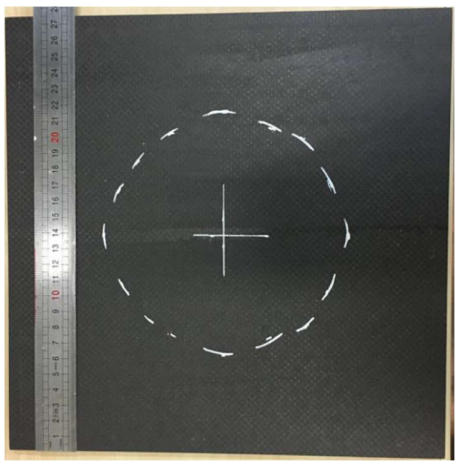

(a): Front view of the sandwich panel

(b): Back view of the sandwich panel

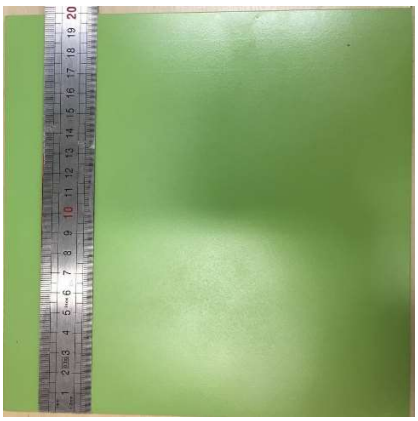

(c): A 200×200 (mm) square aluminum plate

Fig. 2. Photographs of targets.

Projectiles, impact velocity, and impact orientations

The properties of the projectiles, including shape, size, material, and weight are listed in Table 1. The projectiles are provided by the Embraer.

Table 1 – Projectiles shake and dimensions.

Shape	Size (mm)	Weight (g)	Material
Cube	9.5*	~7	Steel

* Tolerance: -0 and +0.3 mm

A valid impact test should meet both velocity and impact orientation criteria. The cubic projectiles must have the initial impact velocity of $213.4^{+5\%}_{-0}$ before the first impact, i.e. impact velocity should be between 213.4 (m/s) and 224.07 (m/s). The cubic projectile must hit the first target at three specific orientations with only $\pm 5^0$ tolerance. These three impact orientations, Corner-On, Edge-On, and Face-On, are introduced in Fig. 3.

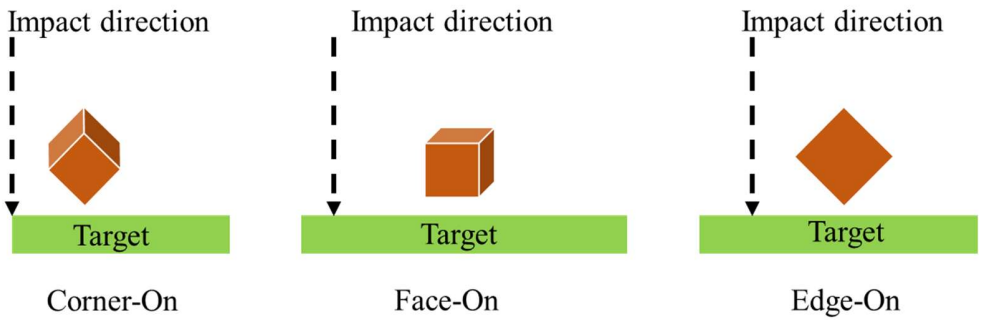

Fig. 3 - Impact orientations.

Impact test setup

Impact tests were conducted using gas gun apparatus at GMSIE-EPUSP. The gun has a 28 (mm) inner diameter barrel that is approximately 2.8 (m) long. There are several holes in the barrel very close to the end of the barrel that relieve the pressure behind the projectile. An Air compressor is used to increase the pressure in the gun pressure vessel. A solenoid valve between the pressure vessel and the gun barrel is used to perform tests. After releasing the air into the barrel, the compressed air accelerates the projectile through the barrel. Figure 4 shows some details of the gas gun apparatus and the schematic presentation of the impact test setup.

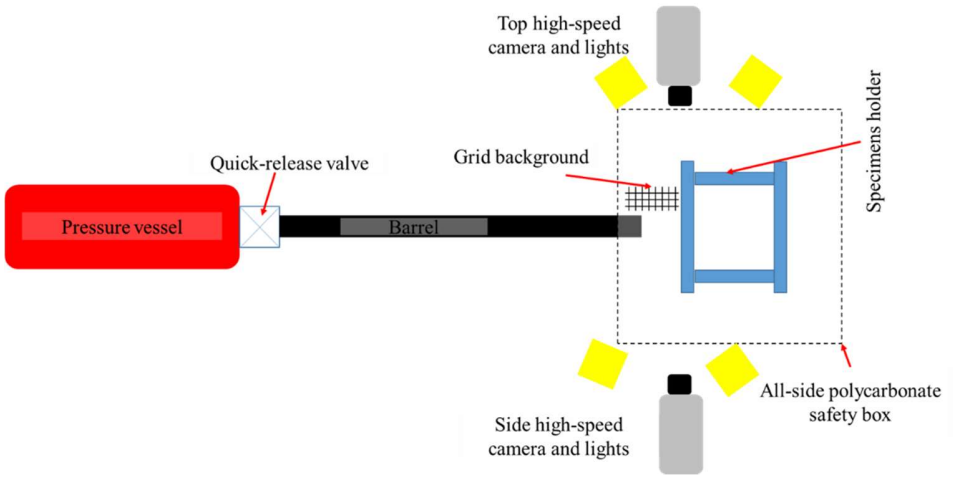

(a): Schematic presentation of gas gun setup

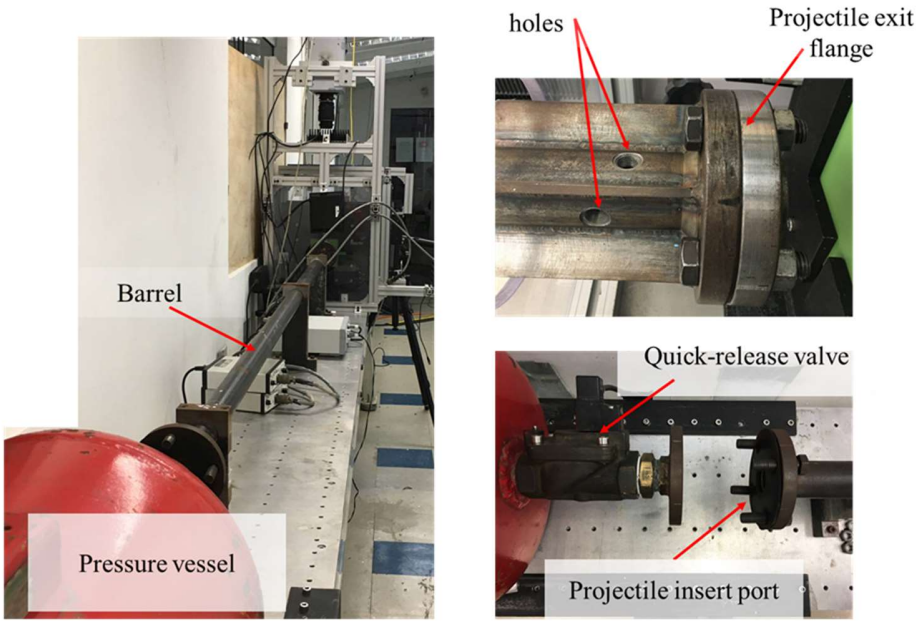

(b): Details of gas gun

Fig. 4- The gas gun setup.

Impact test fixture (plate holders)

The impact test fixture has two plate holders to fix the composite panel and aluminum plate at a constant distance of 200 mm from each other, see Fig. 5. The plate holders are almost identical having a 130×130 mm free impact area for both composite sandwich plane and aluminum plate The plate holders are welded to a horizontal base to fix the test fixture on the table with using several M8 blots to restrict any movement of the fixture due to impact. Specimens were clamped between the plate holder and fixer plates (Fig. 5(b)) by using twelve M8 stainless steel bolts. To increase the local and global rigidity of the fixture, the plate holders were stiffened by several brackets and steel rods (Fig. 5(a)). Fixtures parts, including plate holders, brackets, and base plate are made of steel sheets with a 10 (mm) nominal thickness.

(a): Impact fixture consists of two parallel vertical plate holders (nominal distance 200 mm between plate holders)

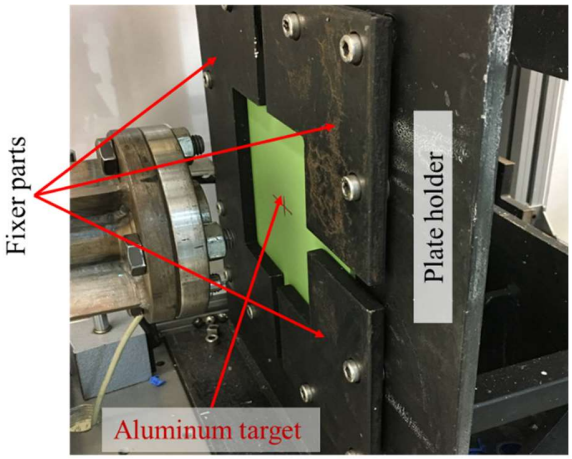

(b): Aluminum plate is mounted on the plate holder

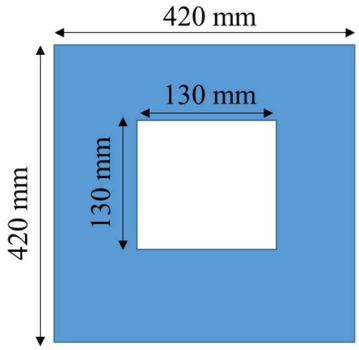

(c): 130 × 130 mm free impact area on the plate holders

Fig. 5 – Impact test fixture.

Since it was required to verify the impact angle of the projectile at the impact initiation point, three small viewports were cut on the fixer plates for both composite and aluminum holders, see Fig. 6.

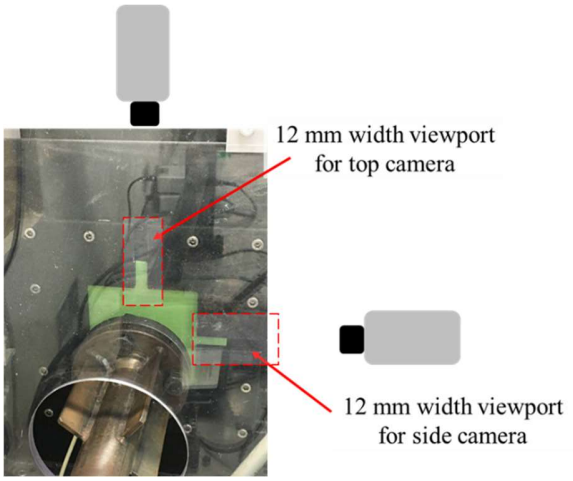

(a): Modified target holder for impact angle verification.

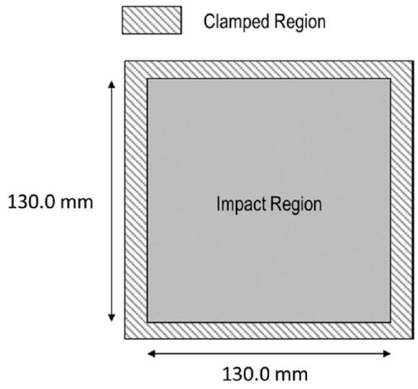

(b): Original target area and clamped region [2].

Fig. 6 – Small viewports on the

Impact velocity measurement and impact angle verification

High-speed images were used to extract the projectile velocity before the impact besides verifying the impact angle of the projectile at the impact initiation point. Thus two orthogonal high-speed cameras were used to record the projectile trajectory. Figure 7 shows the position and distance of cameras from the plate centerlines.

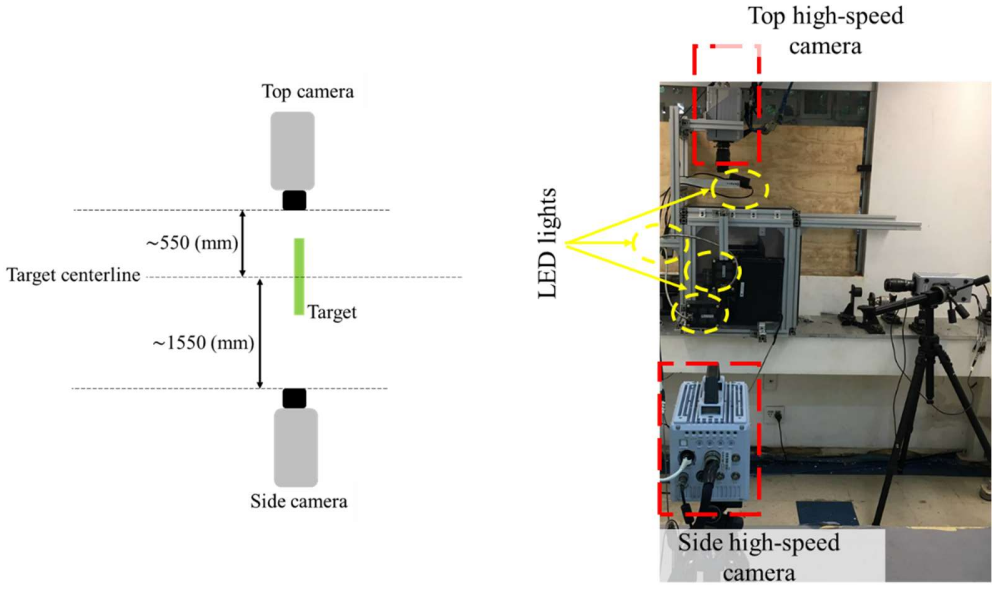

Fig. 7- High-speed camera arrangement.

To align the camera with the center of the barrel, a laser alignment was used to set the center of the camera lens and the center of the barrel at the same height. A digital compass was used to make the camera centerline perpendicular to the plate specimen, Fig. 8.

(a): Finding the normal orientation of the plate mounted on the fixture

(b): Using the straight edge of the camera to find the desired direction

Fig. 8- Setting the camera centerline perpendicular to the plate's normal direction.

Table 2 lists the details of the imaging system. The side high-speed camera was used to measure the initial impact velocity and impact angle at the vertical plane. However, the top high-speed camera was only used to measure the impact angle at the horizontal plane.

Table 2- Details of the imaging system.

Camera ID	Model	Lens	FPS	Application
Side Camera	Photron SASTCAM SA5	100 mm F2.8 MACRO (AT-XM100PROD-TOKINA)	135 kfps	Impact velocity measurement Impact angle verification
Top camera			124- 84 kfps	Impact angle verification

The Photron Fastcam high-speed camera with 135 kfps (equivalent to 135 kHz sampling rate) for all impact tests was used to measure the velocity and impact angle (in the vertical plane) of the projectiles before impact on the first specimen (side camera). Using a high frames-per-second recording speed, the projectile's flight path could be recorded with several frames before and after impact. The camera recording settings required a great deal

of light. The illumination was provided by five special LED lights to record images with reasonable quality. Both top and side cameras were triggered by a signal from an optic sensor located at the exit flange (muzzle) of the gas gun.

Impact angle verification

Since it was mentioned earlier, Cubic projectiles must impact the first specimen with three different orientations; (I) Edge-On, (II) Face-On, and (III) Corner-On, see Fig. 3. A tolerance of ±5° is acceptable for the debris orientations. To launch the cubic projectiles with desired orientations with high accuracy, for each impact angle, a Sabot was designed. Figure 9 presents the Sabots used in the present study. Sabots were manufactured by using a 3D printer.

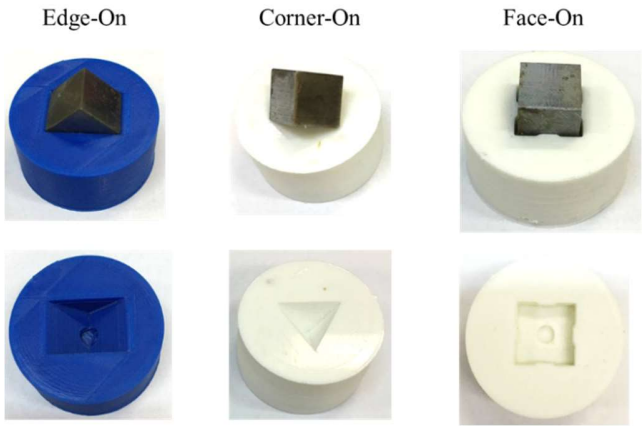

Fig. 9– Sabots for different impact orientations.

Images from high-speed cameras were used to verify the impact orientation tolerance (±5º). The snapshots of high-speed images (both top and side views) were imported into the CAD software and a graphical procedure was followed to verify the impact orientation criterion. Figure 10 explains the impact angle verification procedure briefly. Figure 11 illustrates the impact angle verification of a Corner-On impact test as an example.

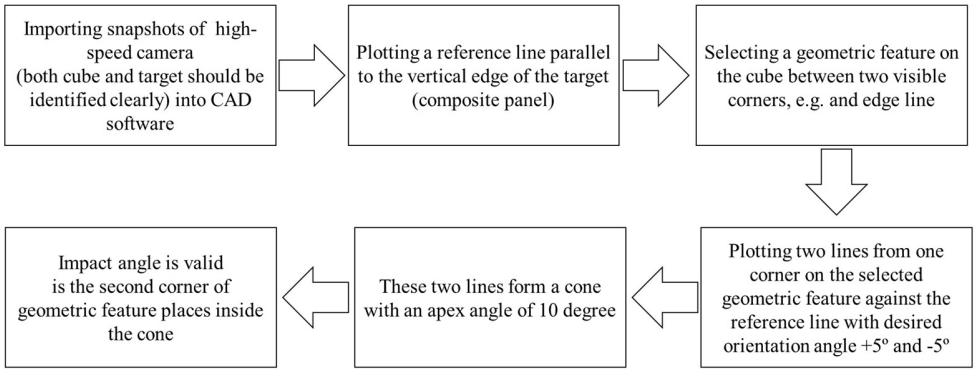

(a): Impact angle verification procedure

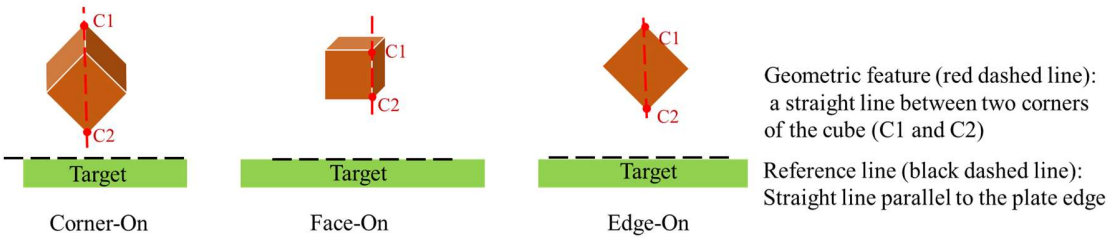

(b): Examples of drawing geometric feature lines and reference lines for different impact angles

Fig. 10. General procedure to check the impact test angle validity.

It is worth noting that due to the dark color of the composite panel, in several pre-tests it was not possible to find the boundary of the composite panel confidently to plot the reference line. Thus, white stickers close to the impact point were placed on the plate specimens (see Fig. 11(a)) to facilitate drawing the reference line parallel to the plate vertical edge.

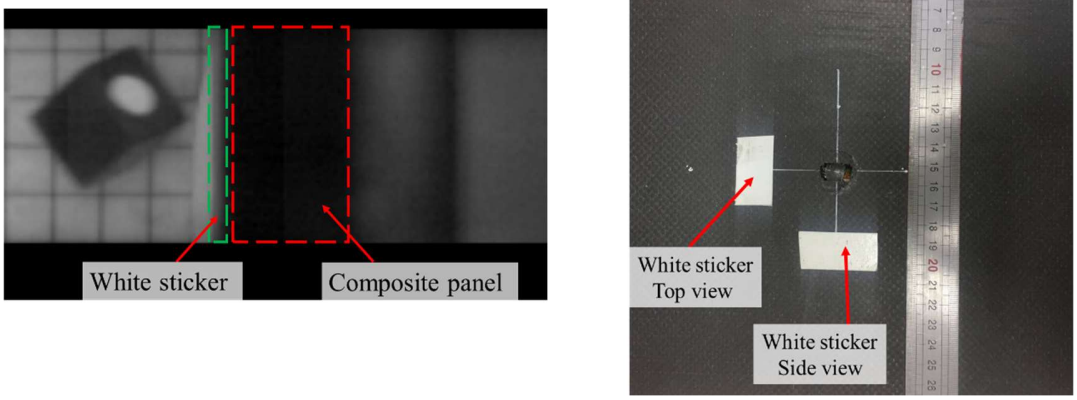

(a): Role and position of the white stickers.

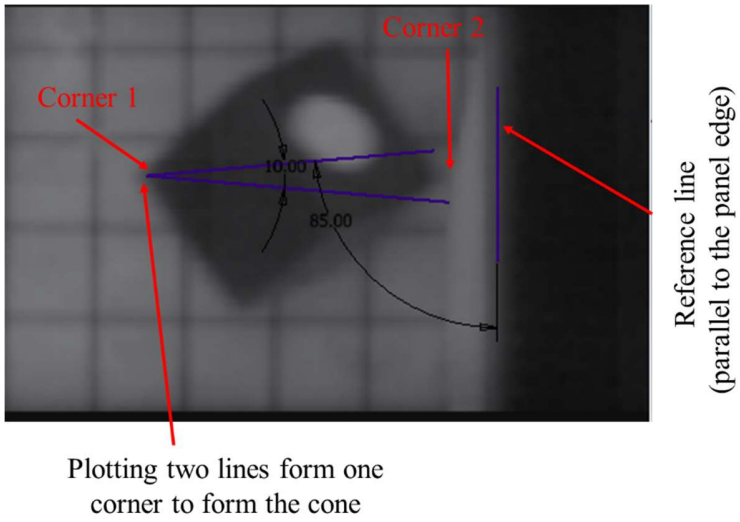

(b): Checking the impact orientation in the vertical plane (side view)

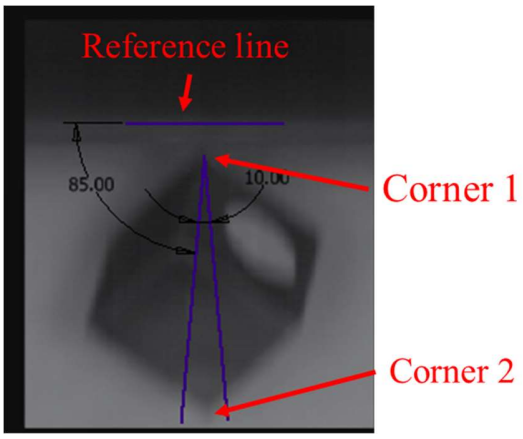

(c): Checking the impact orientation in the horizontal plane (top view)

Fig. 11. Impact orientation check, Corner-On impact is presented as an example.

Initial impact velocity measurement

High-speed images of the side camera were imported to motion tracking software to extract the velocity of the projectile from high-speed images. GOM correlation software was used to measure the velocity of the impactor before the impact. The images were calibrated linearly by using the background grid (having a 5×5 mm dimension). The gird background was placed very close to the projectile path to have a reasonable focus. Figure 12 shows the calibration and velocity measured for a Corner-On impact test using GOM correlation.

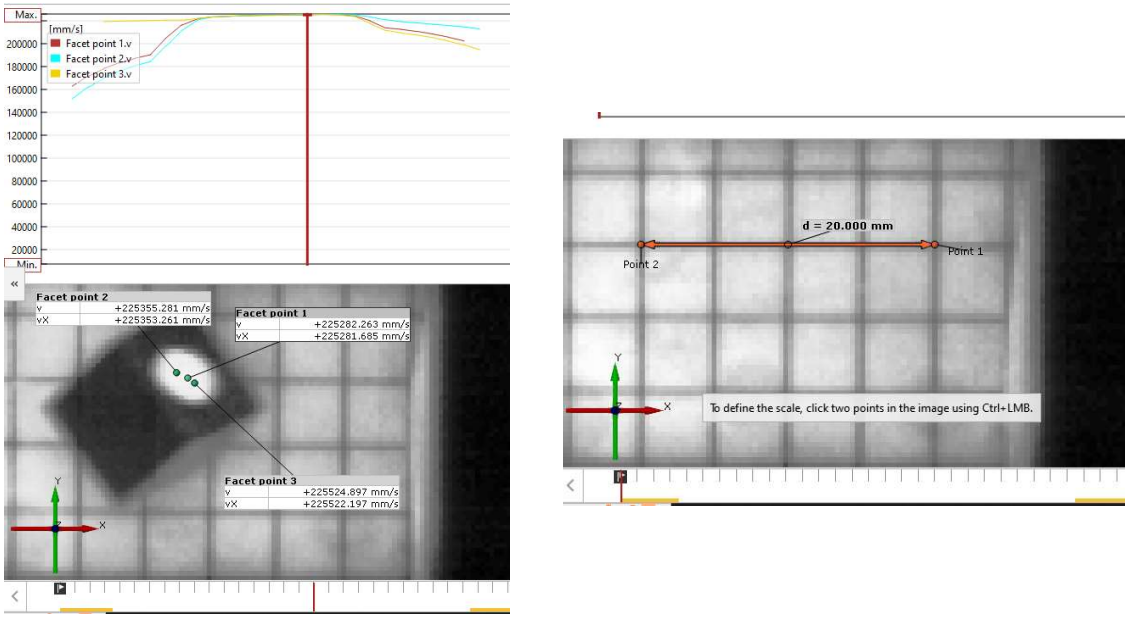

(a) Measured velocity before the impact (b): Linear image calibration

Fig. 12- Velocity measurement from high-speed images.

Leakage test

Right after each impact test, the aluminum plate was removed from the plate holder and assembled on the leakage test fixture, Fig. 13. The leakage test fixture consisted of two identical flat transparent plates (upper and lower) having a hole of 100 (mm) diameter in their center, a rubber gasket, and a long transparent acrylic tube (outer diameter of 100 mm). The

aluminum plate was clamped between the lower and upper plate with eight (or four) M10 bolts tightly. After the bolts were tightened, the tube was filled with water, and the water level reached the 1.4 (m) mark on the tube wall.

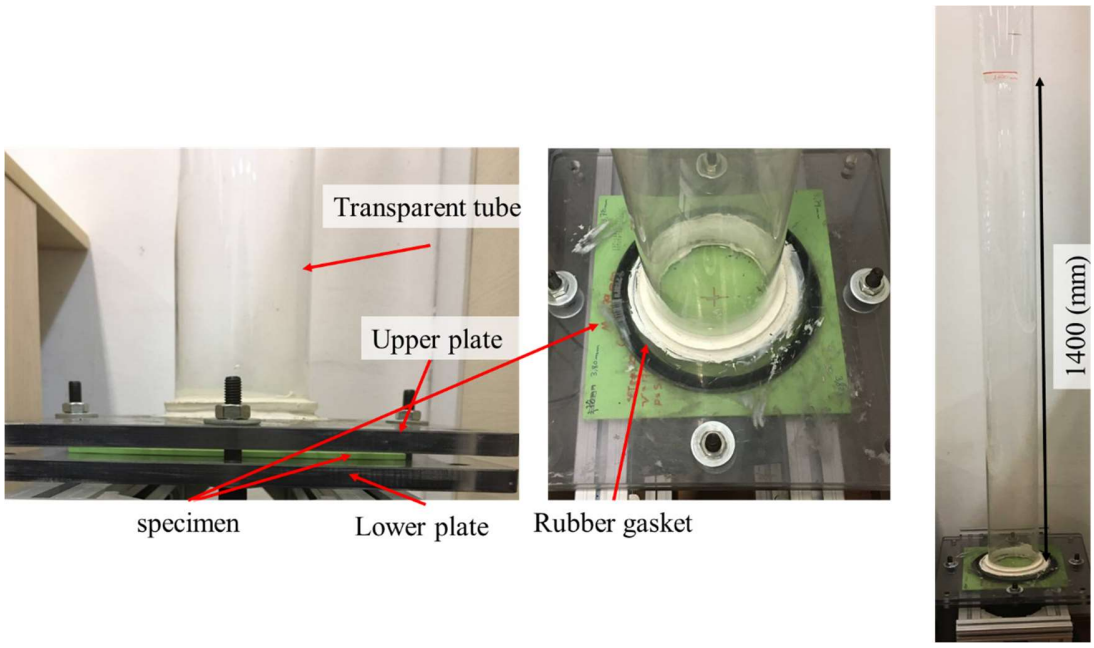

Fig. 13 – The leakage test tank.

Note: The leakage tests were conducted by the Embraer team at the GMSIE laboratory, thus this report does not contain the leakage test results in detail. However, all specimens presented in this report passed the leakage test successfully.

General testing procedure and performance of the proposed setup

Figure 14 explains briefly the test procedure that was followed for each of the tests.

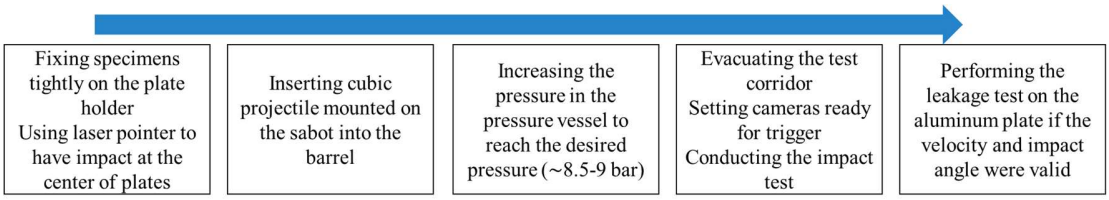

Fig. 14 – General testing procedure.

A comparison between the performance of the present setup and similar ballistic tests on the aluminum plates is presented in Appendix A. Results from Refs. [3] the Edge-On test

with cubic projectile compared to the impact response of aluminum plates having ~3.2 (mm) thick provided by Embraer. Although there are some differences between Ref. [3] and the present investigation, for instance, different boundary conditions, and Aluminum alloys, relatively good agreement between the results of the present study and those reported in Ref. [3] was observed.

Results

Here in this section impact results on the specimens are presented. The leakage tests were performed and registered by the Embraer team, thus, the present report does not cover the leakage results.

Impact test results

Results are removed, only some examples are presented.

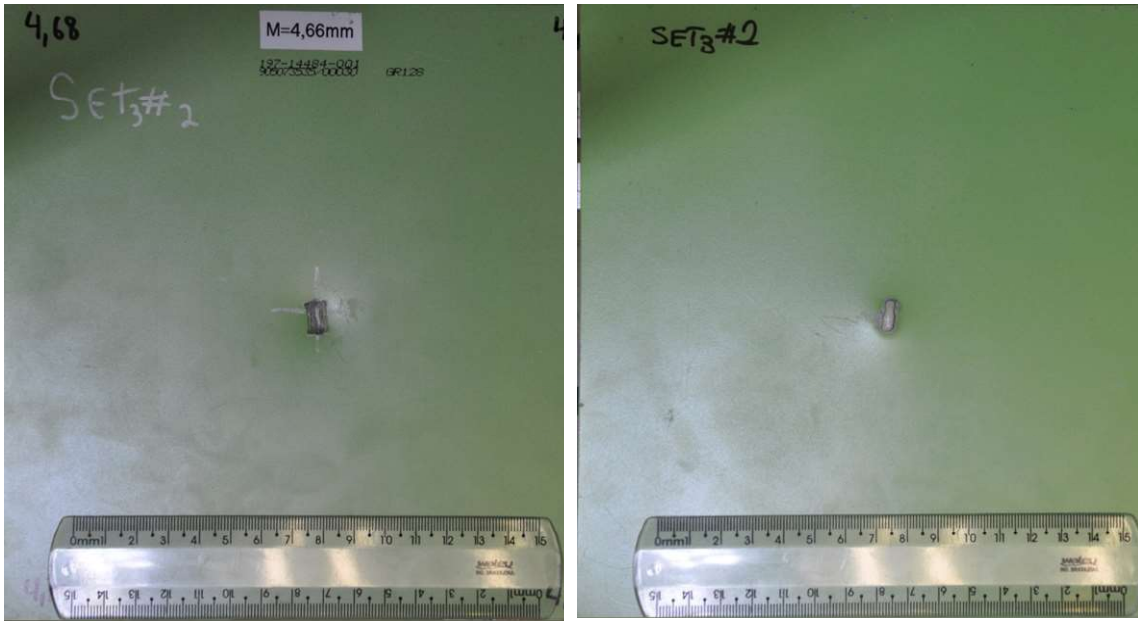

Front view Back view

SET3#2

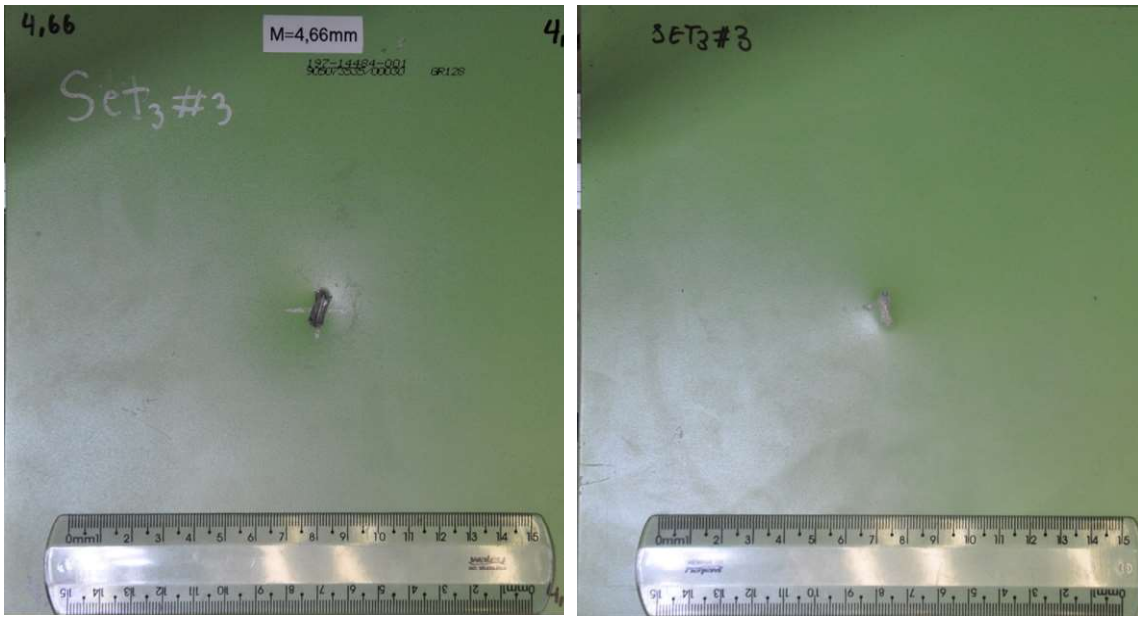

Front view Back view

SET3#3

Fig. 16 – Photographs of post-impact damage inspection, SET3#2 and SET3#3.

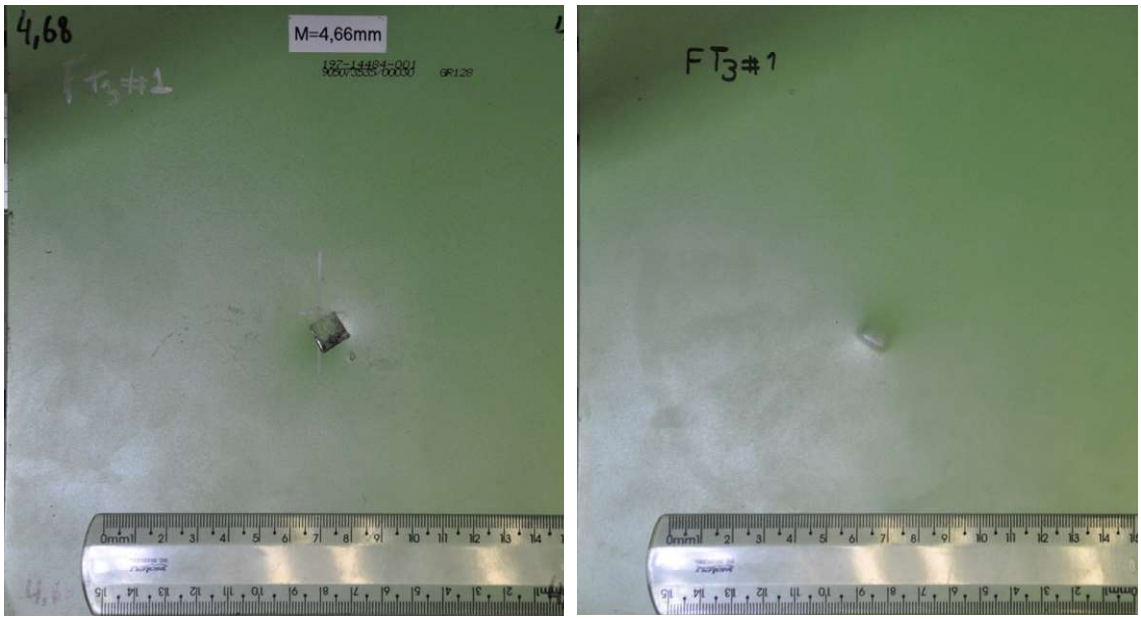

Front view Back view

FT3#1

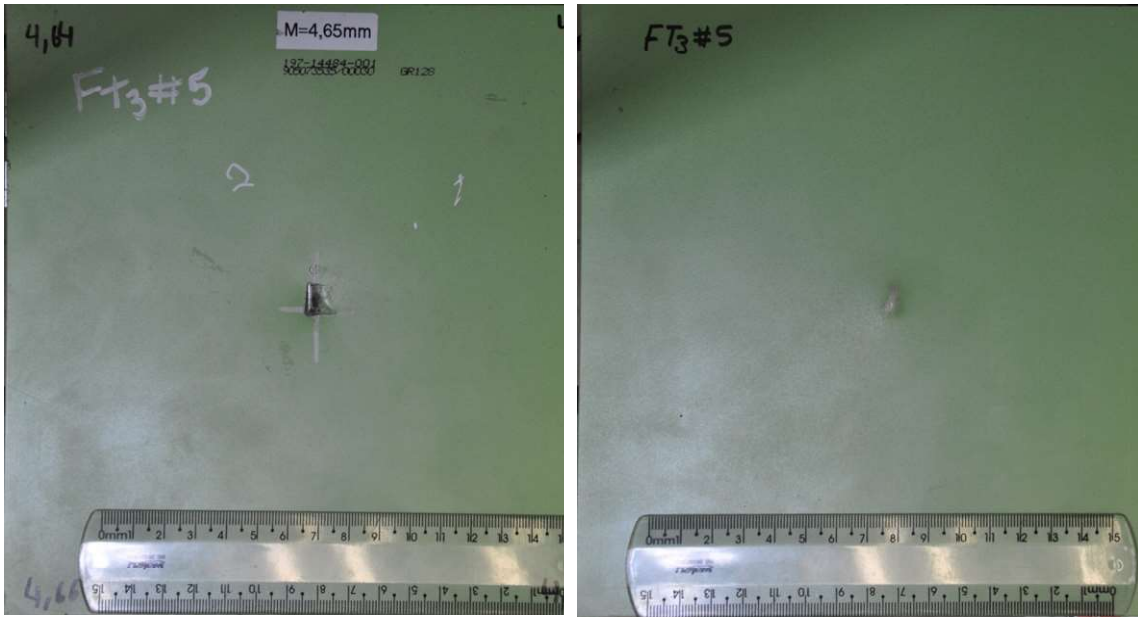

Front view Back view

FT3#5

Fig. 17 – Photographs of post-impact damage inspection, FT3#1 and FT3#5.

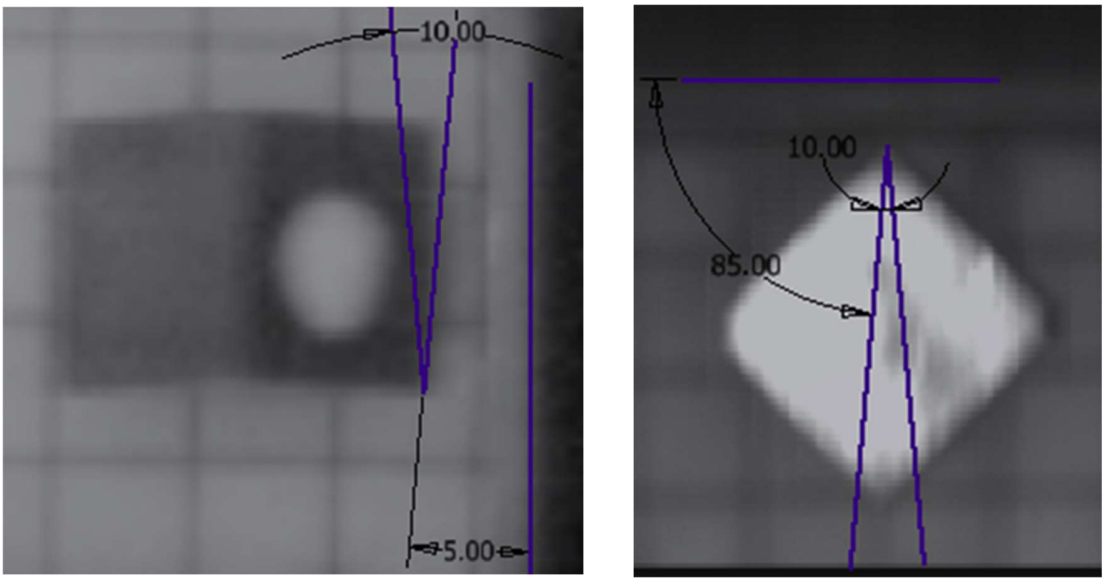

Side view Top view

ET3#7

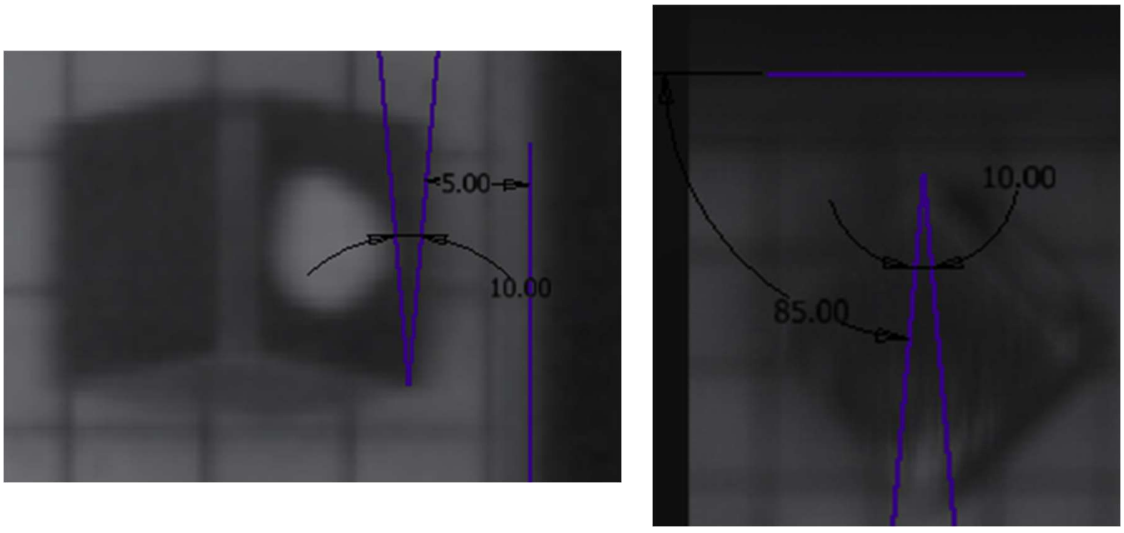

Side view Top view

ET3#4

Fig. 19 – Impact angle verification, ET3#7 and ET3#4

References

1. EMBRAER Technical Report - Fuel tank small debris impact test proposal.
2. EMBRAER Technical Report - Stub Panel Small Debris Impact Test Quotation Request.
3. [1] A. Alavi Nia and J. Haddad Hamedani, "Comparative analysis of energy absorption and deformations of thin walled tubes with various section geometries," *Thin-Walled Struct.*, vol. 48, no. 12, pp. 946–954, Dec. 2010.

[2] X. Lai, Y. Xia, X. Wu, and Q. Zhou, "An experimental method for characterizing friction properties of sheet metal under high contact pressure," *Wear*, vol. 289, pp. 82–94, Jun. 2012.

[3] B. Mussulini, L. Driemeier, R. T. Moura, R. T. Vargas, H. Ramos, and M. Alves, "Slip rate and pressure sensitive friction measurement for crash simulation," *Int. J. Impact Eng.*, vol. 176, p. 104573, Apr. 2023.

[4] W.-R. Chang *et al.*, "The role of friction in the measurement of slipperiness, Part 2: Survey of friction measurement devices," *Ergonomics*, vol. 44, no. 13, pp. 1233–1261, Oct. 2001.

[5] G. Pürçek, T. Savaşkan, T. Küçükömeroğlu, and S. Murphy, "Dry sliding friction and wear properties of zinc-based alloys," *Wear*, vol. 252, no. 11–12, pp. 894–901, Jul. 2002.

[6] J. E. Dunkin and D. E. Kim, "Measurement of static friction coefficient between flat surfaces," *Wear*, vol. 193, no. 2, pp. 186–192, May 1996.

[7] A. Raj, P. Nagarajan, and A. P. Shashikala, "Failure prediction of impact behaviour of self-compacted rubcrete sleepers," *Mater. Des. Process. Commun.*, vol. 3, no. 5, Oct. 2021.

[8] A. M. Remennikov and S. Kaewunruen, "A review of loading conditions for railway track structures due to train and track vertical interaction," *Struct. Control Heal. Monit.*, vol. 15, no. 2, pp. 207–234, Mar. 2008.

[9] S. Kaewunruen and A. M. Remennikov, "Experiments into impact behaviour of

railway prestressed concrete sleepers," *Eng. Fail. Anal.*, vol. 18, no. 8, pp. 2305–2315, Dec. 2011.

[10] W. Ferdous, A. Manalo, G. Van Erp, T. Aravinthan, S. Kaewunruen, and A. Remennikov, "Composite railway sleepers – Recent developments, challenges and future prospects," *Compos. Struct.*, vol. 134, pp. 158–168, Dec. 2015.

[11] G. VAN ERP and M. MCKAY, "Recent Australian Developments in Fibre Composite Railway Sleepers," *Electron. J. Struct. Eng.*, vol. 13, no. 1, pp. 62–66, 2013.

[12] C. Camille, D. Kahagala Hewage, O. Mirza, and T. Clarke, "Full-scale static and single impact testing of prestressed concrete sleepers reinforced with macro synthetic fibres," *Transp. Eng.*, vol. 7, p. 100104, Mar. 2022.

[13] C. Ngamkhanong and S. Kaewunruen, "Effects of under sleeper pads on dynamic responses of railway prestressed concrete sleepers subjected to high intensity impact loads," *Eng. Struct.*, vol. 214, p. 110604, Jul. 2020.

[14] G. Koller, "FFU synthetic sleeper – Projects in Europe," *Constr. Build. Mater.*, vol. 92, pp. 43–50, Sep. 2015.

[15] A. S. Hameed and A. P. Shashikala, "Suitability of rubber concrete for railway sleepers," *Perspect. Sci.*, vol. 8, pp. 32–35, Sep. 2016.

[16] R. V Dukkipati and R. Dong, "Impact Loads due to Wheel Flats and Shells," *Veh. Syst. Dyn.*, vol. 31, no. 1, pp. 1–22, Jan. 1999.

[17] R. N. W. Eriksen, "High Strain Rate Characterisation of Composite Materials," p. 161, 2014.

[18] A. Jadhav, "High Strain Rate Properties of Polymer Matrix Composites," no. August, pp. 1–72, 2003.

[19] K. Zhang, W. Li, Y. Zheng, W. Yao, and C. Zhao, "Compressive Properties and Constitutive Model of Semicrystalline Polyethylene," *Polymers (Basel).*, vol. 13, no. 17, p. 2895, Aug. 2021.

Verification of the performance of the proposed setup

A brief comparison between the results of the direct impact test (without the composite panel) on aluminum plates with ~3.2 (mm) thickness with similar reports in the literature is presented here. Table A.1 lists the descriptions of each test from Ref. [3] and the present study.

Table A.1 – Description of impact test configuration in different studies.

Study	Specimens material	Impactor	Plate thickness (mm)	Boundary condition
Reference [3]	AA2024-T351	Steel cube*	3.175	120×120 (mm) free impact area Only two opposite edges were clamped
Present study	Al 7475-T7351	Steel cube**	~3.2	130×130 (mm) free impact area All four edges were clamped***

* Cubes have a 9.5 (mm) edge length and 6.9 (g) mass
** Cubes have a 9.5 (mm) edge length (tolerance: -0.0 mm +0.3) and ~7 (g) mass
*** Except at small viewports regions

Figure A.1 shows the image tracking by using GOM correlation software before and after the impact of a cube with the Edge-on impact angle. Several snapshots of this impact test were recorded by a camera in the back of the specimen presented in Fig. A.2. Post-impact photos of the specimens in the present study and Ref. [3] for the Edge-On impact test are presented in Fig. A.3. Table A.2 compares the impact velocity and residual velocity between results of the present study and those presented in Ref. [3]. The ballistic limit for this report is not available yet, however, it seems the ballistic limit of the aluminum plate in the present study is about 13% higher than 202 (m/s) presented in Ref. [3]. Considering the slightly better mechanical properties of Al 7475-T7351 (present study) rather than AA2024-T351 (Ref. [3]), the larger free impact area (effect of boundary condition), this difference could be justified.

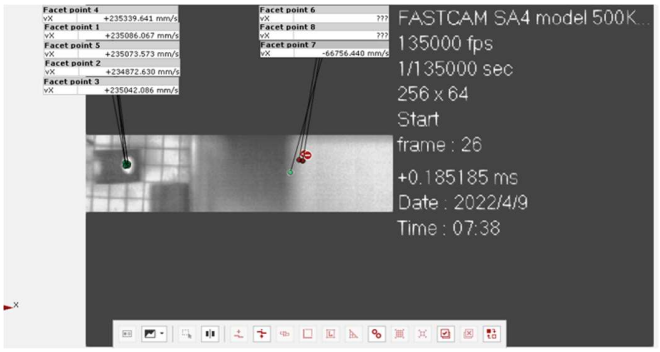

(a): Edge-On impact test on the aluminum plate with 3.2 (mm) thickness (impact angle ~93°), before the impact

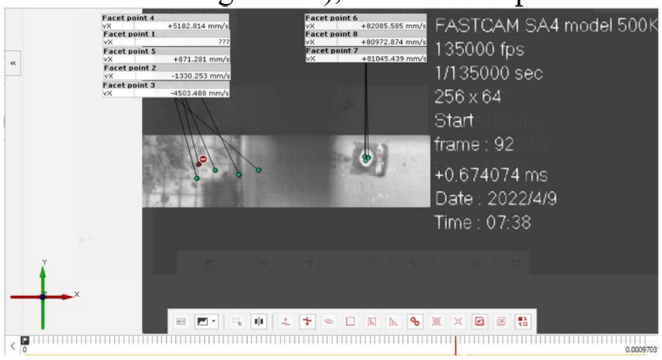

(b): Edge-On impact test on the aluminum plate with 3.2 (mm) thickness (impact angle ~93°), after the impact

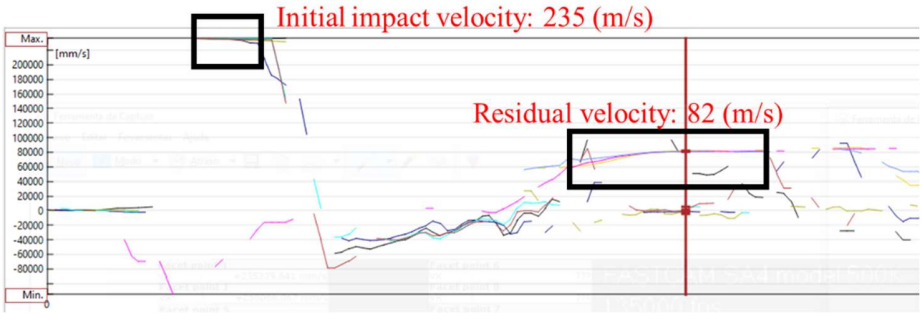

(c): Velocity measurement before and after impact, using high-speed images

Fig. A.1 – Image processing of Edge-on impact in the present verification.

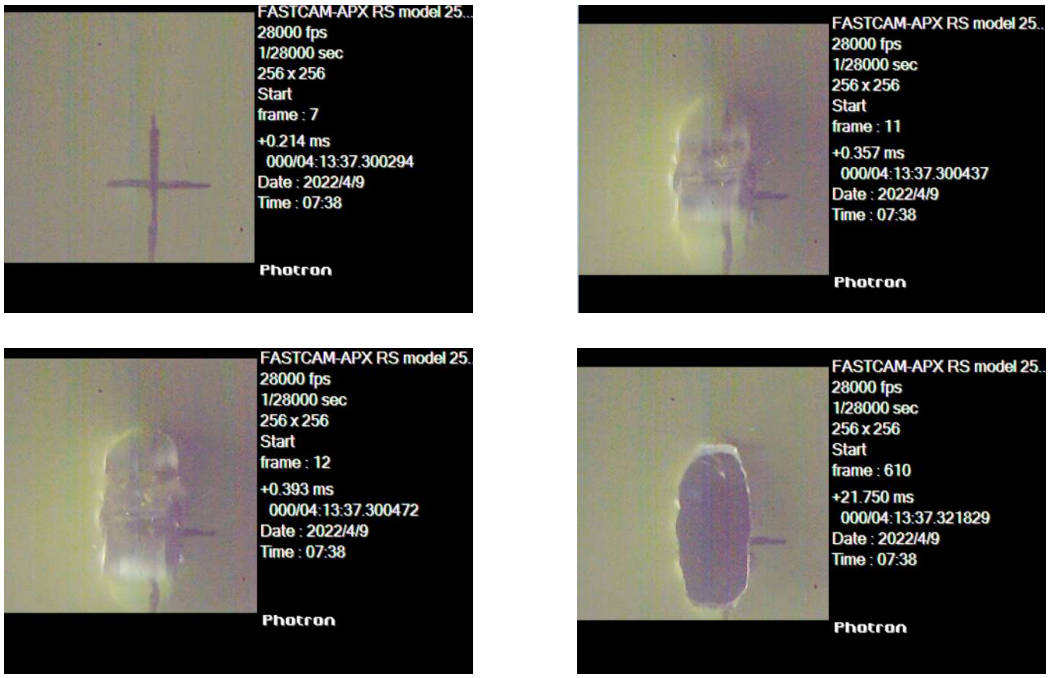

Fig. A.2 – Snapshots from a high-speed camera recording from the back side of the aluminum plate.

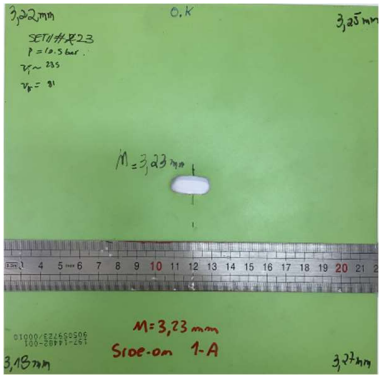

(a): Present study, impact velocity 235 (m/s)

(b): Reference [4], impact velocity 303 (m/s)

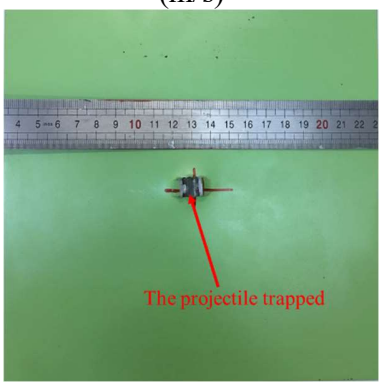

(c): Present study, impact velocity 223 (m/s)

(d): Reference [4], impact velocity 215 (m/s)

Fig. A.3 – Comparison between damages of Edge-On impact in the present study and Ref. [4].

Table A.2 – Comparison between Edge-On impact between Ref. [3] and the present study.

Study	test	Impact velocity (m/s)	Residual velocity (m/s), experimental	Residual velocity (m/s), analytical	V_{50} (m/s), ballistic limit
Ref. [4]	1	198	0	0	202
	2	215	47	54	
	3	**231**	**100**	**88**	
Present study	1	223	0	-	Not available yet
	2	**235**	**82**	-	